Chapter 5
The Divergence of the Casimir Stress

I shall be telling this with a sigh... Two roads diverged in a wood, and I—I took the one less traveled by

Robert Frost, *The Road Not Taken*

5.1 The Casimir Force in Real Media

In the last chapter, we revisited Casimir's original problem of a cavity formed by two perfect mirrors, making a simple modification: an inhomogeneous medium with a continuously varying permittivity profile was introduced into the cavity. Under these conditions, we found that the Casimir-energy of the system, construed as a simple mode summation, can be stated exactly. If this is the case, we might reasonably expect that a generally finite and physically meaningful result can be obtained for systems embodying small-scale inhomogeneities, without incorporating additional information about the microphysical details of their structure.

Nevertheless, Casimir's model—involving a cavity formed by two perfectly reflecting mirrors, which we adopted in our investigation—represents a highly idealised case. There are no perfect mirrors in nature, and real media are both dispersive and dissipative. To predict the behaviour of a realistic physical system, we require a calculus with the capacity to incorporate these phenomena within its description. As discussed in Chap. 2, Lifshitz theory offers such an apparatus [1] that fits fairly well with experimental results [2, 3].

Our aim in this chapter is to repeat our previous thought-experiment, but using a more realistic model involving dispersive dielectric rather than perfect mirrors.[1] The case of macroscopic materials embedded within a fluid is of experimental

[1] The main results in this chapter were published in [4].

W.M.R. Simpson, *Surprises in Theoretical Casimir Physics*, Springer Theses,
DOI 10.1007/978-3-319-09315-4_5

interest [2], and in this case the Casimir force must be computed using the stress tensor within the fluid. In this problem, we seek the value of the force when the fluid is inhomogeneous—for example, when there is a variation in the density of the fluid.[2]

5.2 The Regularised Stress in the Continuum Limit

In Chap. 2, we derived the general form of the stress tensor from which the Casimir forces in a system can be determined. The formalism is written in terms of the electromagnetic Green function, which describes the field produced by charges and currents within the system (2.2.9), (2.2.10). The ground state of the coupled system of electromagnetic field and dielectric is one with non–zero current density within the media [5, 6], consistent with the fluctuation-dissipation theorem [7]. Casimir–Lifshitz forces arise from the interaction of these ground-state currents.

The stress tensor, however, contains the same divergent contribution that appeared in Casimir's original work, and must also be regularised. As we discussed in Sect. 2.3.3, this is typically achieved by subtracting from the total Green function an auxiliary Green function associated with an infinite homogeneous medium [6, 8–11]. One can then compute a finite stress tensor for the system that depends on the dielectric functions of the material at imaginary frequencies. Only then can the force be derived. Both Casimir's and Lifshitz' regularisations give identical results in the limiting case of a cavity sandwiched between perfectly reflecting mirrors.[3]

5.2.1 The Stress Tensor for a Rectangular Cavity

The usual expression for the stress tensor, when applied to a medium that is defined piece–wise along a single axis, is known to be finite.[4] To be explicit, for a region of width a where ϵ and μ are homogeneous, the value of the regularised stress tensor at a point x can be written in terms of the reflection coefficients (as opposed to the Green functions) associated with sending q–polarised ($q = s, p$) plane waves to the right (r_{qR}) and to the left (r_{qL}) of this point [10, 12, 13],

$$\sigma_{xx}(x) = 2\hbar c \sum_{q=s,p} \int_0^\infty \frac{d\kappa}{2\pi} \int_{\mathbb{R}^2} \frac{d^2\boldsymbol{k}_\parallel}{(2\pi)^2} w \frac{r_{qL} r_{qR} e^{-2aw}}{1 - r_{qL} r_{qR} e^{-2aw}}, \tag{5.2.1}$$

[2] For example, sugar dissolved in water under gravity produces an inhomogeneous fluid. This can easily be verified with a laser—light rays entering the fluid become curved.

[3] See Sect. 2.4.2.

[4] Significantly, this is *not* the case for all of the components of the stress tensor: near the boundaries between distinct homogeneous regions, the lateral components of the stress diverge, but the normal component remains finite.

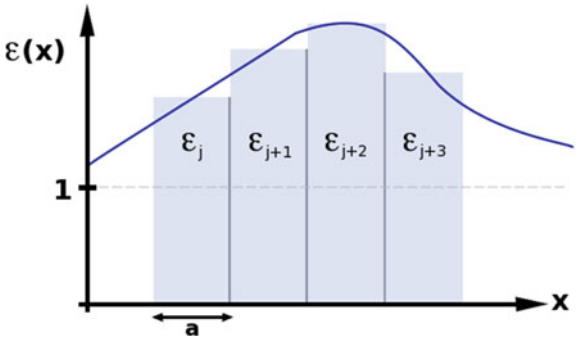

Fig. 5.1 We consider a medium that is inhomogeneous along x, dividing it into N homogeneous slices of width a. The local value of the regularised stress tensor (5.2.1) is then investigated within the medium in the limit as $a \to 0$. For the purposes of illustration only the permittivity $\epsilon(x)$ is shown here. Our analysis holds for both inhomogeneous permittivity and permeability

where $w = (n^2\kappa^2 + k_\parallel^2)^{1/2}$, $k_\parallel = |\boldsymbol{k}_\parallel|$, and n is the value of the refractive index in the homogeneous region surrounding x. The reflection coefficients are functions of the imaginary frequency, $\omega = ic\kappa$, the (real) in–plane wave–vector $\boldsymbol{k}_\parallel$, and the material parameters of the media to the right and to the left of the homogeneous region. This equation is identical to Eq. (2.4.26) which was derived in Sect. 2.4. The advantage of writing the stress tensor in this form is that the regularisation procedure of Lifshitz theory is automatically implemented [10]. The contributions to the stress arise entirely from inhomogeneities in the system. In this chapter we will investigate the behaviour of (5.2.1) in the limit as the piece–wise definition of the medium (see Fig. 5.1) becomes a continuous function ($a \to 0$).

5.2.2 An Anticipated Divergence

Before we proceed with a more lengthy argument, let us consider (5.2.1) in a cavity of width a. This quantity is finite when we integrate over $k_\parallel$ due to the exponential decay of the field across the cavity at imaginary frequencies, the rate of decay becoming increasingly rapid as $k_\parallel$ increases. Indeed, once $k_\parallel$ becomes sufficiently large then the field cannot reach the boundaries of the cavity at all and the reflection coefficients correspondingly tend to zero. However, upon shrinking a, this convergence becomes slower, a higher value of $k_\parallel$ being required before the field fails to make a round trip across the cavity. Given that a continuous medium can be understood as the limit where $a \to 0$, and the refractive index contrast between the cavity and the walls becomes infinitesimal, we should ask whether the reflection coefficients vanish fast enough as $a \to 0$ in order for the stress (5.2.1) to be finite. It seems that they do not: changing variables in (5.2.1) to $\zeta = aw$, and $\xi = ak_\parallel$, we find the whole integral multiplied by a^{-3}. Meanwhile in this limit the reflection coefficients would

in general have contributions linear in a, which would still leave a term proportional to a^{-1} within the stress tensor: a term which diverges in the continuum limit, where $a \to 0$. This remains a suspicion, however. In what follows, we will try to make this argument more precise.

5.3 Transfer Matrices for the Electromagnetic Field

To describe the Casimir stress in an inhomogeneous medium, we will slice it into N homogeneous portions of equal width a, with $Na = L$. In order to evaluate this quantity, we must be able to determine the 'left' and 'right' reflection coefficients of both polarisations, $r_{L\lambda}$ and $r_{R\lambda}$ ($\lambda = 1, 2$), for any slice of the multilayer structure.[5] To achieve this, we must first develop a formalism for tracking the behaviour of the electromagnetic field throughout this structure. In this case, we will deploy the transfer matrix technique for our analysis of the field [13–16]. In what follows, we will derive transfer matrices suitable to our inquiry.

5.3.1 Single-Interface Transfer Matrix

We begin by determining the boundary conditions on the electromagnetic field at a sharp interface between two homogeneous half-spaces.

5.3.1.1 Boundary Conditions for the Electric Field

For the electric field, recalling that $\nabla \cdot \mathbf{D} = 0$, we integrate over a volume such that the boundary sits between its upper and lower surface, where

$$\int_V \nabla \cdot \mathbf{D}\, \mathrm{d}V = 0. \tag{5.3.1}$$

We can shrink the walls of the volume so that all the flux of the field enters or leaves through the top and bottom surfaces, and

$$\int_V \nabla \cdot \mathbf{D}\, \mathrm{d}V = \int \mathbf{D} \cdot \mathrm{d}S \implies \mathbf{D_1} \cdot \hat{\mathbf{x}} \Delta S + \mathbf{D}_2 \cdot \left(-\hat{\mathbf{x}} \Delta S\right) = 0. \tag{5.3.2}$$

[5] This technique may be similarly employed to recover the Green function. See Appendix C.

This determines continuity conditions at the boundary for the normal component of **D**:

$$\mathbf{D}_1 \cdot \hat{\mathbf{x}} = \mathbf{D}_2 \cdot \hat{\mathbf{x}}, \tag{5.3.3}$$

where $\hat{\mathbf{x}}$ is the vector normal to the interface. We can derive conditions for the tangential component of the electric field by applying Faraday's law to a small rectangular loop positioned across the boundary:

$$\int_S \nabla \times \mathbf{E}\, \mathrm{d}S = -\frac{\partial}{\partial t} \int \mathbf{B}\, \mathrm{d}S. \tag{5.3.4}$$

Again, we consider the limiting case where the sides are permitted to contract to zero length, preventing any magnetic flux from cutting the surface, so that

$$\int_S \nabla \times \mathbf{E}\, \mathrm{d}S = \oint \mathbf{E}\, \mathrm{d}l = 0 \implies \int_a^b \mathbf{E}_1 \cdot \mathrm{d}\mathbf{l} + \int_c^d \mathbf{E}_2 \cdot \mathrm{d}\mathbf{l} = 0$$

$$\implies \mathbf{E}_1 \cdot \Delta\mathbf{l} + \mathbf{E}_2 \cdot (-\Delta\mathbf{l}) = 0. \tag{5.3.5}$$

This determines continuity conditions at the boundary for the tangential component of **E**:

$$\mathbf{E}_1 \cdot \hat{\mathbf{t}} = \mathbf{E}_2 \cdot \hat{\mathbf{t}}, \tag{5.3.6}$$

where $\hat{\mathbf{t}}$ is the vector parallel to the interface.

5.3.1.2 Boundary Conditions for the Magnetic Field

We proceed similarly for the magnetic field. Recalling that $\nabla \cdot \mathbf{B} = 0$, we find that

$$\mathbf{B}_1 \cdot \hat{\mathbf{x}} = \mathbf{B}_2 \cdot \hat{\mathbf{x}}. \tag{5.3.7}$$

Recalling that $\nabla \times \mathbf{H} = \frac{\partial \mathbf{D}}{\partial t}$, we also determine that

$$\mathbf{H}_1 \cdot \hat{\mathbf{t}} = \mathbf{H}_2 \cdot \hat{\mathbf{t}}. \tag{5.3.8}$$

In summary, the boundary conditions for the electromagnetic field at an interface between two planar media are such that

1. the in-plane components[6] of **E** and **H** are continuous across the interface.
2. the normal components[7] of **D** and **B** are continuous across the interface.

[6] i.e. the components that lie in a plane parallel to the plane of the interface, and therefore orthogonal to the plane of incidence.

[7] i.e. the components that are normal to the interface.

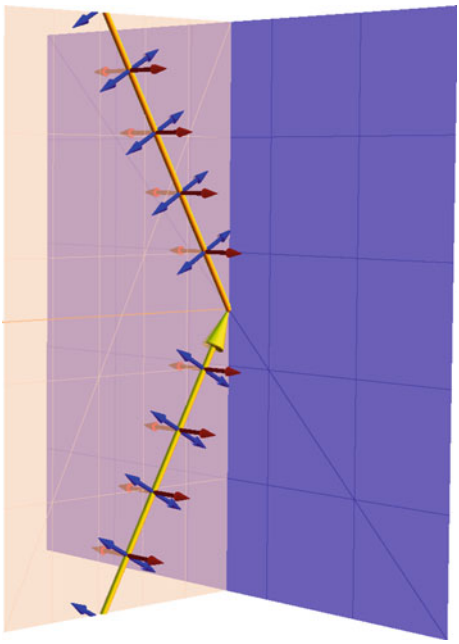

Fig. 5.2 Reflection in the plane. The incident wave-vector $\mathbf{k_1}$ (the *yellow arrow*) strikes an interface and is partially reflected. The incident and reflected wave-vectors both lie in the plane of incidence. Two polarisations are depicted: the *blue arrows* depict the polarisation in which the electric field lies parallel to the plane of incidence; the *red arrows* depict the polarisation that lies orthogonal to it

5.3.1.3 *s* and *p* Polarisations

We consider two polarisations of the electromagnetic field separately. Conventionally, we separate the field into one polarisation in which the waves have electric field orthogonal to the plane of incidence (the plane of the incident and reflected waves), and another in which the electric field lies parallel to it (i.e. the magnetic field is orthogonal to the plane of incidence). We refer to these as s and p polarisations respectively. Because of the linearity of Maxwell's equations, an arbitrary sum of the two polarisations is the solution for a general plane wave (Fig. 5.2).

5.3.1.4 Boundary Conditions Applied to the Electric Field

Consider a single interface between two media: medium 1 $\{\epsilon_1, \mu_1, n_1 = \sqrt{\epsilon_1 \mu_1}\}$ and medium 2 $\{\epsilon_2, \mu_2, n_2 = \sqrt{\epsilon_2 \mu_2}\}$. Real media are dispersive,[8] so the permittivities and permeabilities are functions of the frequency ω. We can write an expression for the field in medium 1, for a given frequency ω, in terms of the s and p polarisations for waves propagating forwards and backwards:

$$\mathbf{E}_1 = E_{1s}^{(+)}(\mathbf{x})\mathbf{e}_{1s}^{(+)} + E_{1s}^{(-)}(\mathbf{x})\mathbf{e}_{1s}^{(-)} + E_{1p}^{(+)}(\mathbf{x})\mathbf{e}_{1p}^{(+)} + E_{1p}^{(-)}(\mathbf{x})\mathbf{e}_{1p}^{(-)}. \tag{5.3.9}$$

[8] Dissipation is incorporated by including an imaginary component in the refractive index.

The orientations of the s and p waves are given by the unit vectors

$$\mathbf{e}_{1s}^{(\pm)} = \hat{\mathbf{x}} \times \hat{\mathbf{k}}_{\parallel}, \tag{5.3.10a}$$

$$\mathbf{e}_{1p}^{(\pm)} = \hat{\mathbf{k}_1}^{(\pm)} \times \mathbf{e}_{1s}^{(\pm)}, \tag{5.3.10b}$$

where $\mathbf{k}_1^{(\pm)} = \pm k_{1x}\hat{\mathbf{x}} + \mathbf{k}_{\parallel}$, $\hat{\mathbf{x}}$ is a unit vector normal to the interface, k_{1x} is the component of the wave-vector normal to the interface, and $\hat{\mathbf{k}}_{\parallel} = \mathbf{k}_{\parallel}/k_{\parallel}$ defines a plane parallel to the interface.[9] Applying the continuity of the in-plane part of the electric field across the two interfaces,[10]

$$\mathbf{E}_1 \cdot \mathbf{e}_{1s}^{(\pm)} = \mathbf{E}_2 \cdot \mathbf{e}_{2s}^{(\pm)}, \tag{5.3.11}$$

$$\mathbf{E}_1 \cdot \hat{\mathbf{k}}_{\parallel} = \mathbf{E}_2 \cdot \hat{\mathbf{k}}_{\parallel}, \tag{5.3.12}$$

yields the equations

$$E_{1s}^{(+)} + E_{1s}^{(-)} = E_{2s}^{(+)} + E_{2s}^{(-)}, \tag{5.3.13}$$

$$\frac{k_{1x}}{n_1}\left[E_{1p}^{(+)} - E_{1p}^{(-)}\right] = \frac{k_{2x}}{n_2}\left[E_{2p}^{(+)} - E_{2p}^{(-)}\right], \tag{5.3.14}$$

having noted[11] that

$$\mathbf{e}_{1p}^{(\pm)} \cdot \mathbf{e}_{1s}^{(\pm)} = 0, \quad \hat{\mathbf{k}}_{\parallel} \cdot \mathbf{e}_{1s}^{(\pm)} = 0, \quad \hat{\mathbf{k}}_{\parallel} \cdot \mathbf{e}_{1p}^{(\pm)} = \mp\frac{ck_{1x}}{n_1\omega}. \tag{5.3.15}$$

Then, applying continuity for the normal component of the displacement field,

$$\mathbf{D}_1 \cdot \hat{\mathbf{x}} = \mathbf{D}_2 \cdot \hat{\mathbf{x}}, \tag{5.3.16}$$

we obtain

$$\frac{\epsilon_1}{n_1}\left[E_{1p}^{(+)} + E_{1p}^{(-)}\right] = \frac{\epsilon_2}{n_2}\left[E_{2p}^{(+)} + E_{2p}^{(-)}\right], \tag{5.3.17}$$

having noted[12] that

---

[9] By definition, a polarisation aligned with $\mathbf{e}_{1s}^{(\pm)}$ excludes any normal component that crosses the interface; the electric field is therefore orthogonal to the plane of incidence. By definition, a polarisation aligned with $\mathbf{e}_{1p}^{(\pm)}$ lies in an orthogonal plane to any polarisation aligned with $\mathbf{e}_{1s}^{(\pm)}$.

[10] This involves two projections, as there are two orthogonal polarisations that we wish to treat separately, each of which contains a component in the plane parallel to the interface.

[11] For the third identity:

$$\hat{\mathbf{k}}_{\parallel} \cdot \mathbf{e}_{1p}^{(\pm)} = \hat{\mathbf{k}}_{\parallel} \cdot \left(\hat{\mathbf{k}_1}^{(\pm)} \times \mathbf{e}_{1s}^{(\pm)}\right) = \frac{\mathbf{k}_{\parallel}}{k} \cdot \left\{\left(\pm k_{1x}\mathbf{x} + \mathbf{k}_{\parallel}\right) \times \left(\hat{\mathbf{x}} \times \hat{\mathbf{k}}_{\parallel}\right)\right\} = \mp\frac{k_{1x}}{k} = \mp\frac{ck_{1x}}{n_1\omega}.$$

[12] For this identity:

$$\hat{\mathbf{x}} \cdot \mathbf{e}_{1p}^{(\pm)} = \frac{ck_\parallel}{n_1 \omega}. \tag{5.3.18}$$

There is no similar contribution for the s component, whose field is orthogonal to the plane of incidence, $\hat{\mathbf{x}} \cdot \mathbf{e}_{1s}^{(\pm)} = 0$, and therefore has no normal component across the interface.

5.3.1.5 Boundary Conditions Applied to the Magnetic Field

We determine the magnetic field via

$$i\omega \mathbf{B}_1 = \nabla \times \mathbf{E}_1, \tag{5.3.19}$$

which implies

$$\mathbf{B}_1 = \frac{n_1}{c}\left[E_{1s}^{(+)}(\mathbf{x})\mathbf{e}_{1p}^{(+)} + E_{1s}^{(-)}(\mathbf{x})\mathbf{e}_{1p}^{(-)} - E_{1p}^{(+)}(\mathbf{x})\mathbf{e}_{1s}^{(+)} - E_{1p}^{(-)}(\mathbf{x})\mathbf{e}_{1s}^{(-)}\right]. \tag{5.3.20}$$

The continuity of $\mathbf{k}_\parallel \cdot \mathbf{H}$ gives the boundary condition

$$\frac{k_{1x}}{\mu_1}\left[E_{1s}^{(+)} - E_{1s}^{(-)}\right] = \frac{k_{2x}}{\mu_2}\left[E_{2s}^{(+)} - E_{2s}^{(-)}\right]. \tag{5.3.21}$$

Applying the remaining conditions on the magnetic field does not generate any new equations.

5.3.1.6 The Component Transfer Matrices

From the four equations obtained by applying the boundary conditions, we can form the matrix equation

$$\begin{pmatrix} 1 & 1 & 0 & 0 \\ \frac{k_{1x}}{\mu_1} & -\frac{k_{1x}}{\mu_1} & 0 & 0 \\ 0 & 0 & \frac{\epsilon_1}{n_1} & \frac{\epsilon_1}{n_1} \\ 0 & 0 & \frac{k_{1x}}{n_1} & -\frac{k_{1x}}{n_1} \end{pmatrix} \begin{pmatrix} E_{1s}^{(+)} \\ E_{1s}^{(-)} \\ E_{1p}^{(+)} \\ E_{1p}^{(-)} \end{pmatrix} = \begin{pmatrix} 1 & 1 & 0 & 0 \\ \frac{k_{2x}}{\mu_2} & -\frac{k_{2x}}{\mu_2} & 0 & 0 \\ 0 & 0 & \frac{\epsilon_2}{n_2} & \frac{\epsilon_2}{n_2} \\ 0 & 0 & \frac{k_{2x}}{n_2} & -\frac{k_{2x}}{n_2} \end{pmatrix} \begin{pmatrix} E_{2s}^{(+)} \\ E_{2s}^{(-)} \\ E_{2p}^{(+)} \\ E_{2p}^{(-)} \end{pmatrix}. \tag{5.3.22}$$

Clearly, the s and p polarisations are not coupled and can be treated separately. For the s polarisation

$$\hat{\mathbf{x}} \cdot \mathbf{e}_{1p}^{(\pm)} = \frac{1}{k_1}\hat{\mathbf{x}} \cdot \left\{\pm k_{1x}\mathbf{x} \times \mathbf{e}_{1s}^{(\pm)} + \mathbf{k}_\parallel \times \left(\hat{\mathbf{x}} \times \hat{\mathbf{k}}_\parallel\right)\right\} = \frac{k_\parallel}{k_1}\hat{\mathbf{x}} \cdot \left\{\hat{\mathbf{k}}_\parallel \times \left(\hat{\mathbf{x}} \times \hat{\mathbf{k}}_\parallel\right)\right\} = \frac{ck_\parallel}{n_1\omega}.$$

$$\begin{pmatrix} 1 & 1 \\ \frac{k_{1x}}{\mu_1} & -\frac{k_{1x}}{\mu_1} \end{pmatrix} \begin{pmatrix} E_{1s}^{(+)} \\ E_{1s}^{(-)} \end{pmatrix} = \begin{pmatrix} 1 & 1 \\ \frac{k_{2x}}{\mu_2} & -\frac{k_{2x}}{\mu_2} \end{pmatrix} \begin{pmatrix} E_{2s}^{(+)} \\ E_{2s}^{(-)} \end{pmatrix}. \tag{5.3.23}$$

Rewriting this expression, to express the field quantities on the right in terms of the field quantities on the left, we obtain:

$$\begin{pmatrix} E_{2s}^{(+)} \\ E_{2s}^{(-)} \end{pmatrix} = \frac{\mu_2}{2k_{2x}} \begin{pmatrix} \frac{k_{2x}}{\mu_2} + \frac{k_{1x}}{\mu_1} & \frac{k_{2x}}{\mu_2} - \frac{k_{1x}}{\mu_1} \\ \frac{k_{2x}}{\mu_2} - \frac{k_{1x}}{\mu_1} & \frac{k_{2x}}{\mu_2} + \frac{k_{1x}}{\mu_1} \end{pmatrix} \begin{pmatrix} E_{1s}^{(+)} \\ E_{1s}^{(-)} \end{pmatrix}.$$

Similarly, for the p polarisation:

$$\begin{pmatrix} E_{2p}^{(+)} \\ E_{2p}^{(-)} \end{pmatrix} = \frac{n_2}{2n_1\epsilon_2 k_{2x}} \begin{pmatrix} \epsilon_1 k_{2x} + \epsilon_2 k_{1x} & \epsilon_1 k_{2x} - \epsilon_2 k_{1x} \\ \epsilon_1 k_{2x} - \epsilon_2 k_{1x} & \epsilon_1 k_{2x} + \epsilon_2 k_{1x} \end{pmatrix} \begin{pmatrix} E_{1p}^{(+)} \\ E_{1p}^{(-)} \end{pmatrix}.$$

Thus for an arbitrary interface, composed of a homogeneous medium on one side with dielectric properties ϵ_l and μ_l, and a second homogeneous medium on the other side with properties ϵ_r and μ_r, it follows that the s and p transfer matrices connecting the field across the boundary between the two media are

$$\mathbf{t}_s(l,r) = \frac{1}{2\mu_l k_{xr}} \begin{pmatrix} \mu_l k_{xr} + \mu_r k_{xl} & \mu_l k_{x\,r} - \mu_r k_{xl} \\ \mu_l k_{xr} - \mu_r k_{xl} & \mu_l k_{x\,r} + \mu_r k_{xl} \end{pmatrix}, \tag{5.3.24}$$

$$\mathbf{t}_p(l,r) = \frac{n_r}{2n_l\epsilon_r k_{xr}} \begin{pmatrix} \epsilon_l k_{xr} + \epsilon_r k_{xl} & \epsilon_l k_{xr} - \epsilon_r k_{xl} \\ \epsilon_l k_{xr} - \epsilon_2 k_{xl} & \epsilon_l k_{xr} + \epsilon_r k_{xl} \end{pmatrix}. \tag{5.3.25}$$

We will be considering a stack of homogeneous media of equal width a, indexed by the parameter m. Consequently, we also require the transfer matrix associated with the propagation of a field through a homogeneous slice, in which the field accumulates a phase of $e^{ik_{xm}a}$:

$$\Lambda(m) = \begin{pmatrix} e^{ik_{xm}a} & 0 \\ 0 & e^{-ik_{xm}a} \end{pmatrix}. \tag{5.3.26}$$

5.3.1.7 Imaginary Frequencies

In order to compute the Casimir stress or force integrals, we work in imaginary frequencies: $\omega \to ic\kappa$. This transforms the wave vector:

$$\omega^2 = \frac{c^2}{n^2}k^2 = \frac{c^2}{n^2}\left(k_x^2 + k_\parallel^2\right) \implies k_x = \sqrt{\frac{n^2\omega^2}{c^2} - k_\parallel^2} \to i\sqrt{n^2\kappa^2 + k_\parallel^2}. \tag{5.3.27}$$

We then denote the imaginary wave number

$$w_m = \sqrt{n_m^2 \kappa^2 + k_\parallel^2}. \tag{5.3.28}$$

At imaginary frequency, the transfer matrices are

$$\mathbf{t}_s(l,r) = \frac{1}{2\mu_l w_r} \begin{pmatrix} \mu_l w_r + \mu_r w_l & \mu_l w_r - \mu_r w_l \\ \mu_l w_r - \mu_r w_l & \mu_l w_r + \mu_r w_l \end{pmatrix}, \tag{5.3.29a}$$

$$\mathbf{t}_p(l,r) = \frac{n_r}{2n_l \epsilon_r w_r} \begin{pmatrix} \epsilon_l w_r + \epsilon_r w_l & \epsilon_l w_r - \epsilon_r w_l \\ \epsilon_l w_r - \epsilon_r w_l & \epsilon_l w_r + \epsilon_r w_l \end{pmatrix}. \tag{5.3.29b}$$

The permittivities ϵ and permeabilities μ are now evaluated at imaginary frequencies:

$$\epsilon(\omega) \to \epsilon(i\kappa), \quad \mu(\omega) \to \mu(i\kappa), \quad n(\omega) \to n(i\kappa). \tag{5.3.30}$$

These quantities are obtained from the dielectric properties for real frequencies by Hilbert transformation, but remain real-valued on the imaginary axis. The propagation matrix transforms to

$$\Lambda(m) = \begin{pmatrix} e^{-w_m a} & 0 \\ 0 & e^{w_m a} \end{pmatrix}, \tag{5.3.31}$$

which is also real.

5.3.2 Multilayer Transfer Matrix and Reflection Coefficients

Our intention is to track the properties of the electromagnetic field through an inhomogeneous medium, by modelling the medium as a stack of homogeneous slices. To this end, we seek to construct 'multilayer transfer matrices' that track wave propagation across multiple interfaces:

$$\mathbf{T}_\lambda(l,r) = \prod_{m=l}^{r-1} \Lambda(m+1)\mathbf{t}_\lambda(m,m+1). \tag{5.3.32}$$

This object connects the field emerging from the far right-hand side of a stack of homogeneous slices to the incident field impinging upon the stack in slice l:

$$\begin{pmatrix} E_{r\lambda}^{(+)} \\ E_{r\lambda}^{(-)} \end{pmatrix} = \mathbf{T}_\lambda(l,r) \begin{pmatrix} E_{l\lambda}^{(+)} \\ E_{l\lambda}^{(-)} \end{pmatrix} = \begin{pmatrix} T_{11} & T_{12} \\ T_{21} & T_{22} \end{pmatrix} \begin{pmatrix} E_{l\lambda}^{(+)} \\ E_{l\lambda}^{(-)} \end{pmatrix}. \tag{5.3.33}$$

We can now define the reflection coefficients for an interface composed of multiple slices. If we imagine a wave of unit amplitude incident from the left onto a planar object represented by $\mathbf{T}$, then the field emerging on the far right, into empty or

homogeneous space, will consist only of right-propagating waves. It follows that:

$$\begin{pmatrix} T_{11} & T_{12} \\ T_{21} & T_{22} \end{pmatrix} \begin{pmatrix} 1 \\ r_r \end{pmatrix} = \begin{pmatrix} t_r \\ 0 \end{pmatrix}, \tag{5.3.34}$$

where t_r is the amplitude of the wave emerging on the right-hand side of this structure, and r_r is the amplitude of the wave reflected back. This reflection coefficient is completely determined by the details of the structure contained in the total transfer matrix:

$$T_{21} + T_{22} r_r = 0 \implies r_r = -\frac{T_{21}}{T_{22}}. \tag{5.3.35}$$

Similarly, for a wave incident from the right:

$$\begin{pmatrix} T_{11} & T_{12} \\ T_{21} & T_{22} \end{pmatrix} \begin{pmatrix} 0 \\ t_l \end{pmatrix} = \begin{pmatrix} r_l \\ 1 \end{pmatrix}. \tag{5.3.36}$$

The reflection coefficient is again determined completely by the total transfer matrix.

$$T_{22} t_l = 1 \implies t_l = 1/T_{22} \implies r_l = \frac{T_{12}}{T_{22}}. \tag{5.3.37}$$

5.3.3 Approximate Transfer Matrices for an Inhomogeneous Medium

5.3.3.1 Restricted Regime

The Casimir stress within a multilayer dielectric stack, for a given slice of the structure, may be expressed in terms of its reflection coefficients (5.2.1). However, numerical computations[13] suggest that the stress of an inhomogeneous structure, modelled as a stack of homogeneous slices, diverges as the number of slices increases (i.e. as we approach the continuum limit, in which the slicing becomes infinitesimally thin). The suspicion is that the divergence takes place in the integral over $k_\parallel$. In order to get an analytic fix on this divergence, we restrict our attention to the regime in which the in-plane wave vector is large in comparison to the refractive index multiplied by the frequency, i.e. where $n\kappa/k_\parallel \ll 1$. This extends from some finite value of $k_\parallel$ to infinity. Under these conditions:

$$w_m = \sqrt{n^2\kappa^2 + k_\parallel^2} = k_\parallel \sqrt{1 + \frac{n^2\kappa^2}{k_\parallel^2}} = k_\parallel \left(1 + \frac{1}{2}\frac{n^2\kappa^2}{k_\parallel^2} + \cdots\right) \sim k_\parallel, \tag{5.3.38}$$

[13] See Sect. 5.4.2.

i.e. the quantity w_m becomes constant throughout the structure. The transfer matrices (5.3.29a, 5.3.29b) can also be simplified:

$$\mathbf{t}_s(l,r) \sim \frac{1}{2\mu_l}\begin{pmatrix}\mu_l+\mu_r & \mu_l-\mu_r\\ \mu_l-\mu_r & \mu_l+\mu_r\end{pmatrix}, \tag{5.3.39a}$$

$$\mathbf{t}_p(l,r) \sim \frac{n_r}{2n_l\epsilon_r}\begin{pmatrix}\epsilon_l+\epsilon_r & \epsilon_l-\epsilon_r\\ \epsilon_l-\epsilon_r & \epsilon_l+\epsilon_r\end{pmatrix}. \tag{5.3.39b}$$

These expressions become increasingly exact as $k_\parallel$ increases. We shall refer to this approximation as the 'high wavenumber regime' (*hw*-regime). Consider an inhomogeneous medium situated in the region $x \in [0, L]$. To describe the Casimir stress in this medium, we will slice it into N portions of width a, with $Na = L$, indexed by m. The slices $m = 0$ and $m = N + 1$ contain free space. Restricting ourselves to the *hw*-regime, we first rewrite the transfer matrices (5.3.39a, 5.3.39b):

$$\mathbf{t}_s(m,m+1) = \begin{pmatrix}1+\frac{\Delta\mu_m}{2\mu_m} & -\frac{\Delta\mu_m}{2\mu_m}\\ -\frac{\Delta\mu_m}{2\mu_m} & 1+\frac{\Delta\mu_m}{2\mu_m}\end{pmatrix}, \tag{5.3.40a}$$

$$\mathbf{t}_p(m,m+1) = \frac{n_{m+1}\epsilon_m}{n_m\epsilon_{m+1}}\begin{pmatrix}1+\frac{\Delta\epsilon_m}{2\epsilon_m} & -\frac{\Delta\epsilon_m}{2\epsilon_m}\\ -\frac{\Delta\epsilon_m}{2\epsilon_m} & 1+\frac{\Delta\epsilon_m}{2\epsilon_m}\end{pmatrix}, \tag{5.3.40b}$$

where

$$\Delta\mu_m = \mu_{m+1} - \mu_m, \quad \Delta\epsilon_m = \epsilon_{m+1} - \epsilon_m. \tag{5.3.41}$$

For propagation between two slices, we first cross a boundary, then propagate a distance a. We may define a composite transfer matrix for this process, beginning with the s polarisation:

$$\tau_s(m+1) = \Lambda(m+1)\,\mathbf{t}_s(m,m+1) = \begin{pmatrix}e^{-k_\parallel a} & 0\\ 0 & e^{k_\parallel a}\end{pmatrix}\begin{pmatrix}1+\frac{\Delta\mu_m}{2\mu_m} & -\frac{\Delta\mu_m}{2\mu_m}\\ -\frac{\Delta\mu_m}{2\mu_m} & 1+\frac{\Delta\mu_m}{2\mu_m}\end{pmatrix}.$$

Multiplying the two matrices, and separating the terms, the composite transfer matrix can be cast in the form

$$\begin{pmatrix}\left\{1+\frac{\Delta\mu_m}{2\mu_m}\right\}e^{-k_\parallel a} & -\frac{\Delta\mu_m}{2\mu_m}e^{-k_\parallel a}\\ -\frac{\Delta\mu_m}{2\mu_m}e^{k_\parallel a} & \left\{1+\frac{\Delta\mu_m}{2\mu_m}\right\}e^{k_\parallel a}\end{pmatrix} = \begin{pmatrix}e^{-k_\parallel a} & 0\\ 0 & e^{k_\parallel a}\end{pmatrix} + \frac{\Delta\mu_m}{2\mu_m}\begin{pmatrix}e^{-k_\parallel a} & -e^{-k_\parallel a}\\ -e^{k_\parallel a} & e^{k_\parallel a}\end{pmatrix}. \tag{5.3.42}$$

Proceeding similarly for the p polarised waves, the composite transfer matrices for the two polarisations can be conveniently rewritten in the form

$$\tau_s(m+1) = \boldsymbol{\alpha} + \frac{\Delta\mu_m}{2\mu_m}\boldsymbol{\beta},$$
$$\tau_p(m+1) = \frac{n_{m+1}\epsilon_m}{n_m\epsilon_{m+1}}\left(\boldsymbol{\alpha} + \frac{\Delta\epsilon_m}{2\epsilon_m}\boldsymbol{\beta}\right), \tag{5.3.43}$$

where

$$\boldsymbol{\alpha} = \begin{pmatrix} e^{-k_\parallel a} & 0 \\ 0 & e^{k_\parallel a} \end{pmatrix}, \quad \boldsymbol{\beta} = \begin{pmatrix} e^{-k_\parallel a} & -e^{-k_\parallel a} \\ -e^{k_\parallel a} & e^{k_\parallel a} \end{pmatrix}. \tag{5.3.44}$$

5.3.3.2 Approximating the Transfer Matrices

Besides working within the *hw*-regime, we may simplify the algebra further by limiting our enquiry to the general case of a weakly inhomogeneous medium. The optical profile of the medium under consideration remains arbitrary; we simply restrict ourselves either to the case of an inhomogeneity that is small in magnitude but fairly rapid in variation, or fairly large in magnitude but only slowly varying. Reflections are the result of inhomogeneities. In the case under consideration, we expect the reflection coefficients and the Casimir stress to be small. If there is a divergence in the Casimir stress for even a weakly varying (that is, a weakly reflective) medium, there is every reason to expect a divergence in a strongly varying (strongly reflective) medium.

First, to calculate the stress in a cell l, we require the reflection coefficients of the cell boundaries, r_l and r_r, and therefore the transfer matrices associated with propagation of waves from cell l throughout the multilayer stack, travelling to the left and to the right. We shall consider a configuration for $N+1$ cells. Consider the left transfer matrix for the s polarisation:

$$\begin{aligned}\mathbf{T}_{Ls} = \prod_{m=1}^{l} \tau_s(m) &= \prod_{m=1}^{l}\left(\boldsymbol{\alpha} + \frac{\Delta\mu_{m-1}}{2\mu_{m-1}}\boldsymbol{\beta}\right) \\ &= \left(\boldsymbol{\alpha} + \frac{\Delta\mu_{l-1}}{2\mu_{l-1}}\boldsymbol{\beta}\right)\left(\boldsymbol{\alpha} + \frac{\Delta\mu_{l-2}}{2\mu_{l-2}}\boldsymbol{\beta}\right)\left(\boldsymbol{\alpha} + \frac{\Delta\mu_{l-3}}{2\mu_{l-3}}\boldsymbol{\beta}\right) + \cdots\end{aligned} \tag{5.3.45}$$

It is not possible to analytically evaluate (5.3.45) unless we make the second approximation we alluded to: it is equivalent to the Born approximation in quantum mechanics, where we assume that scattering is weak [15]. In electromagnetism, this means that the properties of the medium must change slowly as a function of position. Products of the transfer matrices can then be truncated to first order in $\Delta\epsilon$ and $\Delta\mu$ [14]. This approximation is quite well suited to our case, for it is the case where the value of the stress ought to be minimal. Thus for a weakly inhomogeneous medium we may neglect terms that are higher than first-order in $\Delta\mu_i$ and $\Delta\epsilon_i$. It follows that

$$\mathbf{T}_{Ls} \sim \boldsymbol{\alpha}^l + \frac{\Delta\mu_{l-1}}{2\mu_{l-1}}\boldsymbol{\beta}\boldsymbol{\alpha}^{l-1} + \frac{\Delta\mu_{l-2}}{2\mu_{l-2}}\boldsymbol{\alpha}\boldsymbol{\beta}\boldsymbol{\alpha}^{l-2} + \frac{\Delta\mu_{l-3}}{2\mu_{l-3}}\boldsymbol{\alpha}^2\boldsymbol{\beta}\boldsymbol{\alpha}^{l-3} + \cdots$$

$$= \boldsymbol{\alpha}^l + \sum_{m=1}^{l} \frac{\Delta\mu_{l-m}}{2\mu_{l-m}}\boldsymbol{\alpha}^{m-1}\boldsymbol{\beta}\boldsymbol{\alpha}^{l-m}. \tag{5.3.46}$$

It is convenient to reverse and reindex the sum:

$$\mathbf{T}_{Ls} \sim \boldsymbol{\alpha}^l + \sum_{m=0}^{l-1} \frac{\Delta\mu_m}{2\mu_m}\boldsymbol{\alpha}^{l-m-1}\boldsymbol{\beta}\boldsymbol{\alpha}^m. \tag{5.3.47}$$

The matrices in the final lines are then

$$\boldsymbol{\alpha}^l = \begin{pmatrix} e^{-k_\parallel la} & 0 \\ 0 & e^{k_\parallel la} \end{pmatrix}, \tag{5.3.48a}$$

$$\boldsymbol{\alpha}^{l-m-1}\boldsymbol{\beta}\boldsymbol{\alpha}^m = \begin{pmatrix} e^{-k_\parallel la} & -e^{k_\parallel (2m-l)a} \\ -e^{k_\parallel (l-2m)a} & e^{k_\parallel la} \end{pmatrix}. \tag{5.3.48b}$$

Thus the transfer matrix can be written

$$\mathbf{T}_{Ls} = \begin{pmatrix} \left[1 + \sum_{m=0}^{l-1} \frac{\Delta\mu_m}{2\mu_m}\right] e^{-k_\parallel la} & -\sum_{m=0}^{l-1} \frac{\Delta\mu_m}{2\mu_m} e^{-k_\parallel (l-2m)a} \\ -\sum_{m=0}^{l-1} \frac{\Delta\mu_m}{2\mu_m} e^{k_\parallel (l-2m)a} & \left[1 + \sum_{m=0}^{l-1} \frac{\Delta\mu_m}{2\mu_m}\right] e^{k_\parallel la} \end{pmatrix}. \tag{5.3.49}$$

For the transfer matrix associated with propagation through the right-hand side of the structure:

$$\mathbf{T}_{Rs} = \prod_{m=l+1}^{N+1} \tau_s(m) = \prod_{m=l+1}^{N+1} \left(\boldsymbol{\alpha} + \frac{\Delta\mu_{m-1}}{2\mu_{m-1}}\boldsymbol{\beta}\right)$$

$$= \left(\boldsymbol{\alpha} + \frac{\Delta\mu_N}{2\mu_N}\boldsymbol{\beta}\right)\left(\boldsymbol{\alpha} + \frac{\Delta\mu_{N-1}}{2\mu_{N-1}}\boldsymbol{\beta}\right)\left(\boldsymbol{\alpha} + \frac{\Delta\mu_{N-2}}{2\mu_{N-2}}\boldsymbol{\beta}\right) + \cdots \tag{5.3.50}$$

We apply the same approximation:

$$\mathbf{T}_{Rs} \sim \boldsymbol{\alpha}^{N+1-l} + \frac{\Delta\mu_N}{2\mu_N}\boldsymbol{\beta}\boldsymbol{\alpha}^{N-l} + \frac{\Delta\mu_{N-1}}{2\mu_{N-1}}\boldsymbol{\alpha}\boldsymbol{\beta}\boldsymbol{\alpha}^{N-l-1} + \frac{\Delta\mu_{N-2}}{2\mu_{N-2}}\boldsymbol{\alpha}^2\boldsymbol{\beta}\boldsymbol{\alpha}^{N-l-2} + \cdots$$

$$= \boldsymbol{\alpha}^{N+1-l} + \sum_{m=l}^{N} \frac{\Delta\mu_m}{2\mu_m}\boldsymbol{\alpha}^{N-m}\boldsymbol{\beta}\boldsymbol{\alpha}^{m-l}. \tag{5.3.51}$$

The matrices in the final lines are

$$\boldsymbol{\alpha}^{N+1-l} = \begin{pmatrix} e^{-k_\parallel(N+1-l)a} & 0 \\ 0 & e^{k_\parallel(N+1-l)a} \end{pmatrix}, \tag{5.3.52a}$$

$$\boldsymbol{\alpha}^{N-m}\boldsymbol{\beta}\boldsymbol{\alpha}^{m-l} = \begin{pmatrix} e^{-k_\parallel(N-l+1)a} & -e^{-k_\parallel(N+l+1-2m)a} \\ -e^{-k_\parallel(N+l+1-2m)a} & e^{k_\parallel(N-l+1)a} \end{pmatrix}. \tag{5.3.52b}$$

Thus the right-transfer matrix for s polarised light is

$$\mathbf{T}_{Rs} = \begin{pmatrix} \left[1+\sum_{m=1}^{N}\frac{\Delta\mu_m}{2\mu_m}\right]e^{-k_\parallel(N-l+1)a} & -\sum_{m=1}^{N}\frac{\Delta\mu_m}{2\mu_m}e^{-k_\parallel(N+l+1-2m)a} \\ -\sum_{m=1}^{N}\frac{\Delta\mu_m}{2\mu_m}e^{k_\parallel(N+l+1-2m)a} & \left[1+\sum_{m=1}^{N}\frac{\Delta\mu_m}{2\mu_m}\right]e^{k_\parallel(N-l+1)a} \end{pmatrix}. \tag{5.3.53}$$

The form of $\mathbf{T}_{Lp}$ and $\mathbf{T}_{Rp}$, for the p polarisation, can be determined without further calculation from their s counterparts by simply substituting permeability for permittivity and multiplying by the prefactor

$$\frac{n_{N+1}\epsilon_l}{n_l\epsilon_{N+1}}. \tag{5.3.54}$$

We can now state the reflection coefficients, applying the same ratios of the elements of the appropriate transfer matrix as before (5.3.35), (5.3.37). For reflection from the left of s polarised light, we obtain the coefficient

$$r_{Ls}(l) = -\frac{\sum_{m=0}^{l-1}\frac{\Delta\mu_m}{2\mu_m}e^{-k_\parallel(l-2m)a}}{\left[1+\sum_{m=0}^{l-1}\frac{\Delta\mu_m}{2\mu_m}\right]e^{k_\parallel la}} = -\frac{\sum_{m=0}^{l-1}\frac{\Delta\mu_m}{\mu_m}e^{-2k_\parallel(l-m)a}}{\left(2+\sum_{j=0}^{l-1}\frac{\Delta\mu_j}{\mu_j}\right)}. \tag{5.3.55}$$

For reflection from the right of s polarised light, we obtain

$$r_{Rs}(l) = \frac{\sum_{m=1}^{N}\frac{\Delta\mu_m}{2\mu_m}e^{k_\parallel(N+l+1-2m)a}}{\left[1+\sum_{m=1}^{N}\frac{\Delta\mu_m}{2\mu_m}\right]e^{k_\parallel(N-l+1)a}} = \frac{\sum_{m=1}^{N}\frac{\Delta\mu_m}{\mu_m}e^{-2k_\parallel(m-l)a}}{\left[2+\sum_{m=1}^{N}\frac{\Delta\mu_m}{\mu_m}\right]}. \tag{5.3.56}$$

The reflection coefficients of the p polarisation can be recovered by replacing the permeabilities with the permittivities. It is convenient to introduce into all the reflection coefficients an additional phase factor, such that we can associate the reflection coefficients for each slice with a point x_l at the centre of the slice. The complete set of reflection coefficients are then given as follows: for reflection of s and p polarised light from the left,

$$r_{Ls}(x_l) = -\frac{\sum_{m=0}^{l-1} \frac{\Delta\mu_m}{\mu_m} e^{-2k_\parallel(l-m-1/2)a}}{\left(2+\sum_{m=0}^{l-1} \frac{\Delta\mu_m}{\mu_m}\right)},$$
$$r_{Lp}(x_l) = -\frac{\sum_{m=0}^{l-1} \frac{\Delta\epsilon_m}{\epsilon_m} e^{-2k_\parallel(l-m-1/2)a}}{\left(2+\sum_{m=0}^{l-1} \frac{\Delta\epsilon_m}{\epsilon_m}\right)}; \tag{5.3.57}$$

for reflection from the right,

$$r_{Rs}(x_l) = \frac{\sum_{m=l}^{N} \frac{\Delta\mu_m}{\mu_m} e^{-2k_\parallel(m-l+1/2)a}}{\left(2+\sum_{m=l}^{N} \frac{\Delta\mu_m}{\mu_m}\right)},$$
$$r_{Rp}(x_l) = \frac{\sum_{m=l}^{N} \frac{\Delta\epsilon_m}{\epsilon_m} e^{-2k_\parallel(m-l+1/2)a}}{\left(2+\sum_{m=l}^{N} \frac{\Delta\epsilon_m}{\epsilon_m}\right)}. \tag{5.3.58}$$

5.4 The Casimir Stress in an Inhomogeneous Medium

To recapitulate briefly, we have approximated the inhomogeneous medium as a series of N homogeneous strips of width a (see Fig. 5.1). We have employed the transfer matrix technique for our analysis of the field [13–16], with the field in strip $j+1$ being related to that in j by

$$\boldsymbol{E}_q(j+1) = \boldsymbol{t}_q(j+1) \cdot \boldsymbol{E}_q(j), \tag{5.4.1}$$

where the index q labels the polarization as in (5.2.1), and $\boldsymbol{t}_q(j+1)$ is the transfer matrix relating the field on the far right of slice j to that on the far right of slice $j+1$. In (6.2.11) the electric field amplitude, $\boldsymbol{E}_q$ is written as a two element vector containing the right (+) and left (−) going parts,

$$\boldsymbol{E}_q(j) = \begin{pmatrix} E_q^{(+)}(j) \\ E_q^{(-)}(j) \end{pmatrix}. \tag{5.4.2}$$

We number the transfer matrices in (6.2.11) from 1 to $N+1$, with ϵ_0 and ϵ_{N+1} equal to the vacuum permittivity, and μ_0 and μ_{N+1} the vacuum permeability. In each of these slices $\boldsymbol{t}_q$ is given by the usual expression for the transfer matrix in piece–wise homogeneous media (e.g. [14, 16]). For the imaginary frequencies, $\omega/c = i\kappa$, encountered within (5.2.1) the x–directed wave–vector in the jth slice is also imaginary, $k_j = iw_j$, where, $w_j = (n_j^2\kappa^2 + k_\parallel^2)^{1/2}$. The limit of $N \to \infty$ and $a \to 0$ will be taken in the final step of the calculation.

Our object is to apply this formalism to determine whether the stress tensor (5.2.1) remains finite when the properties of the medium are represented by continuous

functions of position. We suspect that it is not: a divergence of (5.2.1) is anticipated in the integral over $k_\parallel = |\boldsymbol{k}_\parallel|$. Physically—considering the allowed modes on the real frequency axis—we can picture this divergent contribution arising due to waves of high $k_\parallel$ undergoing reflections from the inhomogeneity of the medium. As $k_\parallel$ is increased, these waves contribute ever more to the local value of the stress tensor, when presumably in reality they should not be supported by the medium at all. For the purpose of identifying this anticipated divergence, we have restricted our attention to the *hw*-regime of the integrand in (5.2.1), where the in–plane wave–vector is large in comparison to the 'refractive index' multiplied by the 'frequency', $n_j\kappa/k_\parallel \ll 1$.

5.4.1 The High-Wavenumber Divergence

The integral for the Casimir stress, at a position x_l within the multilayer structure, can now be stated in terms of the quantities we have derived:

$$\sigma_{xx}(x_l) = 2\hbar c \sum_{\lambda=s,p} \int_0^\infty \frac{\mathrm{d}\kappa}{2\pi} \int_{\mathbb{R}^2} \frac{\mathrm{d}^2\mathbf{k}_\parallel}{(2\pi)^2} w \frac{r_{L\lambda}(x_l) r_{R\lambda}(x_l) e^{-2aw}}{1 - r_{L\lambda}(x_l) r_{R\lambda}(x_l) e^{-2aw}}, \tag{5.4.3}$$

where

$$w = \sqrt{n(x_l, i\kappa)^2\kappa^2 + k_\parallel^2}, \quad k_\parallel = \left|\mathbf{k}_\parallel\right|, \tag{5.4.4}$$

and the reflection coefficients $r_{s\lambda}$ are defined by (5.3.57), (5.3.58). $n(i\kappa)$ is the refractive index of slice l evaluated at imaginary frequencies. To examine the behaviour of the stress in the integral over $k_\parallel$ we evaluate the integrand above at fixed κ (that is, for a fixed frequency) and therefore at $n(x_l) = n(x_l, i\kappa)$. A semi-infinite part of the integral over $k_\parallel$ is taken in the regime of high wave numbers $[K, \infty)$, where $w \sim k_\parallel$. The quantity we wish to analyse is

$$I = \sum_{\lambda=s,p} \int_K^\infty \frac{\mathrm{d}k_y}{2\pi} \int_K^\infty \frac{\mathrm{d}k_z}{2\pi} k_\parallel \frac{r_{L\lambda} r_{R\lambda} e^{-2k_\parallel a}}{1 - r_{L\lambda} r_{R\lambda} e^{-2k_\parallel a}}. \tag{5.4.5}$$

It is convenient to rewrite the integral in polar coordinates:

$$\sum_{\lambda=s,p} \int_0^{2\pi} \frac{\mathrm{d}\theta}{2\pi} \int_K^\infty \frac{k_\parallel^2 \mathrm{d}k_\parallel}{2\pi} \frac{r_{L\lambda} r_{R\lambda} e^{-2k_\parallel a}}{1 - r_{L\lambda} r_{R\lambda} e^{-2k_\parallel a}}. \tag{5.4.6}$$

If this quantity is divergent, then the stress integral as a whole is divergent. This is true regardless of the absorbing properties of the medium, or its frequency dispersion profile. We can expand the denominator in the expression above in a series of

ascending powers of the reflection coefficients, on the assumption that $r_{L\lambda}r_{R\lambda}e^{-2k_\parallel a} < 1$, so that this sum converges for all a and all $k_\parallel$:

$$r_{L\lambda}r_{R\lambda}e^{-2k_\parallel a}\left(1 - r_{L\lambda}r_{R\lambda}e^{-2k_\parallel a}\right)^{-1} = r_{L\lambda}r_{R\lambda}e^{-2k_\parallel a}\left[1 + r_{L\lambda}r_{R\lambda}e^{-2k_\parallel a} + \left(r_{L\lambda}r_{R\lambda}e^{-2k_\parallel a}\right)^2 + \cdots\right], \tag{5.4.7}$$

which can be written more concisely as

$$\sum_{n=0}\left(r_{L\lambda}r_{R\lambda}e^{-2k_\parallel a}\right)^{n+1}. \tag{5.4.8}$$

We may now rewrite I and introduce the quantity $I_{\lambda n}$:

$$I = \frac{1}{2\pi}\sum_{n=0}^{\infty}\sum_{\lambda=s,p} I_{\lambda n}, \quad I_{\lambda n} = \int_K k_\parallel^2 \mathrm{d}k_\parallel \left(r_{L\lambda}r_{R\lambda}\right)^{n+1} e^{-2(n+1)k_\parallel a}. \tag{5.4.9}$$

Consider the quantity $I_{s0} = \int_K^\infty k_\parallel^2 \mathrm{d}k_\parallel r_{Ls}r_{Rs}e^{-2k_\parallel a}$. First, we insert the expressions for the reflection coefficients:

$$I_{s0} = -\int_K^\infty k_\parallel^2 \mathrm{d}k_\parallel \frac{\sum_{m=0}^{l-1}\sum_{m'=l}^{N}\frac{\Delta\mu_m\Delta\mu_{m'}}{\mu_m\mu_{m'}}e^{-2k_\parallel(m'-m+1)a}}{\left(2+\sum_{m=0}^{l-1}\frac{\Delta\mu_m}{\mu_m}\right)\left(2+\sum_{m'=l}^{N}\frac{\Delta\mu_{m'}}{\mu_{m'}}\right)}. \tag{5.4.10}$$

The integral over $k_\parallel$ can now be evaluated. It is an integral of the form[14]

$$\int x^2e^{cx}\mathrm{d}x = \frac{\partial^2}{\partial c^2}\int e^{cx}\mathrm{d}x = \frac{\partial^2}{\partial c^2}\left[\frac{1}{c}e^{cx}\right] = e^{cx}\left(\frac{x^2}{c} - \frac{2x}{c^2} + \frac{2}{c^3}\right). \tag{5.4.11}$$

Putting $c = -2\left(m'-m\right)a$, and integrating over $k_\parallel$, we obtain

$$\int_K^\infty \mathrm{d}k_\parallel k_\parallel^2 e^{-2k_\parallel(m'-m+1)a} = K_0\, e^{-2K(m'-m+1)a} \tag{5.4.12}$$

where

$$K_0 = \left(\frac{K^2}{2(m'-m+1)a} + \frac{2K}{4(m'-m+1)^2a^2} + \frac{2}{8(m'-m+1)^3a^3}\right). \tag{5.4.13}$$

[14] We have set the constant of integration to zero.

Thus the integral I_{s0} evaluates as

$$I_{s0} = -\frac{\sum_{m=0}^{l-1}\sum_{m'=l}^{N}\frac{\Delta\mu_m\Delta\mu_{m'}}{\mu_m\mu_{m'}}K_0\,e^{-2K(m'-m+1)a}}{\left(2+\sum_{m=0}^{l-1}\frac{\Delta\mu_m}{\mu_m}\right)\left(2+\sum_{m'=l}^{N}\frac{\Delta\mu_{m'}}{\mu_{m'}}\right)}. \tag{5.4.14}$$

In fact, this quantity can be made arbitrarily large by slicing the medium more finely—that is, by decreasing the width of each slice by increasing the number of slices. To see this, we consider the quantity I_{s0} in the continuum limit. First, we rewrite the sums as integrals:

$$\sum_{m=0}^{l-1} \to \int_0^x \mathrm{d}x_1, \quad \sum_{m'=l}^{N} \to \int_x^L \mathrm{d}x_2. \tag{5.4.15}$$

The terms involving the permeabilities can be reexpressed as logarithms.

$$\frac{\Delta\mu_m}{\mu_m} = \frac{\mu_{m+1}-\mu_m}{\mu_m} \to \frac{1}{\mu(x_1)}\frac{\mathrm{d}}{\mathrm{d}x_1}\mu(x_1) = \frac{\mathrm{d}}{\mathrm{d}x_1}\ln\left[\mu(x_1)\right], \tag{5.4.16}$$

Similarly,

$$\frac{\Delta\mu_{m'}}{\mu_{m'}} \to \frac{\mathrm{d}}{\mathrm{d}x_2}\ln\left[\mu(x_2)\right]. \tag{5.4.17}$$

The sums on the denominator of (5.4.14) becomes integrals that can be straightforwardly evaluated:

$$\begin{aligned}\int_0^x \mathrm{d}x_1\frac{\mathrm{d}}{\mathrm{d}x_1}\ln\left[\mu(x_1)\right] &= \ln\left[\mu(x)\right] - \ln\left[\mu(0)\right],\\ \int_x^L \mathrm{d}x_2\frac{\mathrm{d}}{\mathrm{d}x_2}\ln\left[\mu(x_2)\right] &= \ln\left[\mu(L)\right] - \ln\left[\mu(x)\right].\end{aligned} \tag{5.4.18}$$

Since the medium is situated in a vacuum, $\ln\left[\mu(0)\right] = \ln\left[\mu(L)\right] = \ln 1 = 0$. Finally, we arrive at an expression for (5.4.14) in the continuum limit: I_{s0} is equal to

$$-\left(2+\ln\left[\mu(x_1)\right]\right)^{-1}\left(2-\ln\left[\mu(x_2)\right]\right)^{-1}\int_0^x \mathrm{d}x_1\int_x^L \mathrm{d}x_2\frac{\mathrm{d}}{\mathrm{d}x_1}\ln\left[\mu(x_1)\right]\frac{\mathrm{d}}{\mathrm{d}x_2}\ln\left[\mu(x_2)\right]$$
$$\left(\frac{K^2}{2(x_2-x_1)a}+\frac{2K}{4(x_2-x_1)^2a^2}+\frac{2}{8(x_2-x_1)^3a^3}\right)e^{-2K(x_2-x_1)a}. \tag{5.4.19}$$

This expression clearly diverges. It therefore seems that there is no finite continuum limit of the regularised stress tensor (5.2.1). Including the additional terms in the series (5.4.9) will not affect this result [4]. Whilst these contributions diverge in a similar manner, they represent higher powers of the derivatives of ϵ and μ—terms that vary quite independently as the spatial dependence of ϵ and μ is changed, and therefore cannot be expected to cancel in general. As the remainder of the integral over $\boldsymbol{k}_\parallel$ is finite, we conclude that the whole integral diverges as $a \to 0$. Consequently (5.2.1) diverges everywhere within an inhomogeneous medium described by ϵ and μ that are continuous functions of position. This is independent of how these quantities depend on imaginary frequency.

5.4.2 A Numerical Illustration

The divergence demonstrated analytically above was first spotted numerically when attempting to compute a stress profile for a system similar to the one in [9], and the results of these numerical computations serve to illustrate the argument. For the sake of simplicity we consider an impedance-matched system $\epsilon = \mu = n$ with the refractive index profile

$$n(x) = \begin{cases} 3 & x \leq 0, \\ 3\,\mathrm{e}^{-x} & 0 < x < \mathrm{Log}\,3, \\ 1 & x \geq \mathrm{Log}\,3. \end{cases} \tag{5.4.20}$$

The system contains an imhomogeneous region between $x = 0$ and $x = \mathrm{Log}\,3$. In order to investigate the properties of this system using the transfer matrix technique described earlier (but dispensing with the approximations introduced in Sect. 5.3.3), we divide the inhomogeneous region into N homogeneous pieces (see Fig. 5.3), and determine the left and right reflection coefficients within each piece. It is then possible

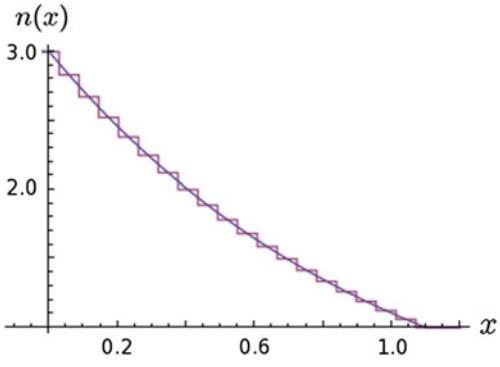

Fig. 5.3 The continuous refractive index profile of the system, and a piece–wise approximation using 20 homogeneous slices

to calculate the local value of the regularised stress. The formula for the stress (5.2.1) can be rewritten more simply in this case [10], noting that the coefficients depend only on the magnitude of the wave vector components, and not on the angle between them[15]:

$$\sigma = \frac{\hbar c}{\pi^2} \int_0^\infty \int_0^\infty k_\parallel w \frac{r_L r_R \mathrm{e}^{-2aw}}{1 - r_L r_R \mathrm{e}^{-2aw}} dk_\parallel \, d\kappa. \tag{5.4.21}$$

As N becomes large (i.e. as the cavity width a becomes small), the approximation becomes increasingly accurate. *Prima facie*, there should be little to distinguish the physics of the case $N = 400$ from the case $N = 800$, as both approximations of the continuum case are now very smooth. Nevertheless, as Fig. 5.4 shows, the stress (though regularised) increases markedly, and it continues to grow as more slices are added. Why is this happening? Plots of the integrand of the stress (6.2.7), where the wave number $k_\parallel$ and the number of slices N are allowed to vary, show that the integral falls off less and less rapidly with $k_\parallel$ as N is increased (Fig. 5.5).

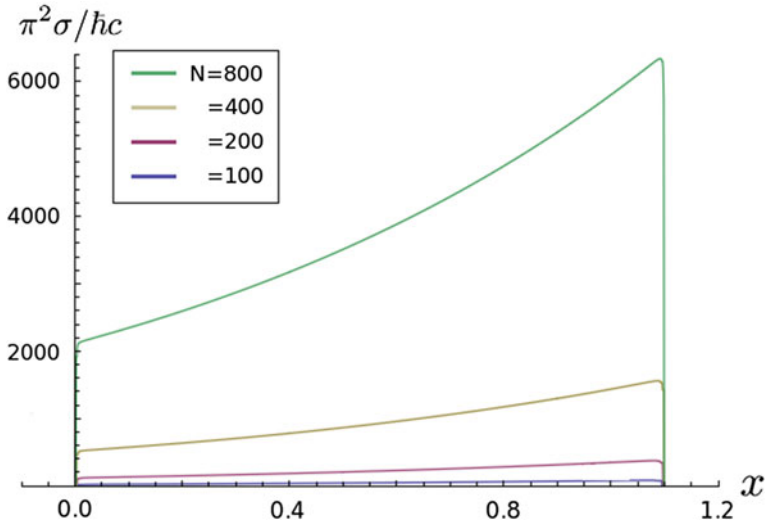

Fig. 5.4 The medium, inhomogeneous between $x = 0$ and $x = \mathrm{Log}\, 3$, is divided into 100, 200, 400 and 800 homogeneous slices. The local absolute value of the regularised stress tensor (6.2.7)—normalised in units of $\hbar c/\pi^2$—is plotted for each case at a given position x. The stress increases as the number of divisions increases

[15] We also note that the electric and magnetic coefficients are equal, due to impedance-matching, and hence need not be referred to separately.

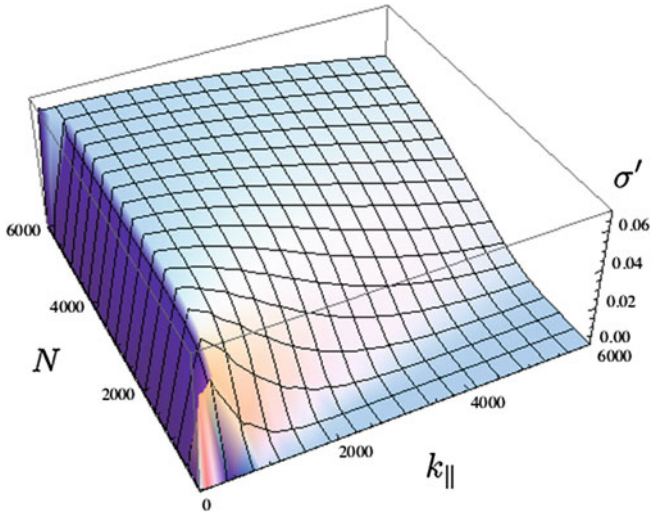

Fig. 5.5 The integrand of the stress (6.2.7), σ', (normalised in the same units as Fig. 5.4) is plotted for $\kappa = 1$ at the centre of the system, with $k_\parallel$ varying from $k_\parallel = 1$ to $k_\parallel = 6,000$ (horizontal axis), and N ranging from $t = 10$ to $t = 6,000$ (depth axis). As the number of slices N is increased, the integrand falls off less rapidly with $k_\parallel$, and thus the integral of the stress converges less rapidly

5.4.3 Speculations on Spatial Dispersion

We might wonder how finite results ought to be extracted from this formalism. The advantage of the usual regularisation procedure is that it removes an infinite quantity that does not depend on the inhomogeneity of the medium, which cannot be relevant to the force. Conversely, here we have a divergent contribution that is due to the inhomogeneity of the medium. The divergence originates within the fact that the reflection coefficients (5.3.57), (5.3.58) do not go to zero fast enough as $k_\parallel \to \infty$ in the limit where $a \to 0$.

One approach to this problem might be to terminate the integral over $k_\parallel$ at some finite cut–off. However, the value of this cut–off would seem to be arbitrary. Alternatively, before the continuum limit is taken, we might just remove some small region of the sum around the point where $k - j = 1$, although the size of this region would also be arbitrary. This problem is reminiscent of that found in the case of spontaneous emission within an absorbing dielectric, where an additional physical parameter—equivalent to removing a portion of the dielectric in the immediate vicinity of the atom—must be introduced in order to obtain a finite emission rate [17, 18].

However, it might be urged that the solution to this problem involves the recognition that, as with other problems in physics, the specific dependence of the dielectric media on both the frequency *and* the wave vector ought to be included within the macroscopic description of matter, at the level of the electric permittivity and magnetic permeability functions. It is a familiar thought that realistic models of

macroscopic media must include the phenomenon of *temporal* dispersion: in linear and causal time-independent systems, this amounts to the acknowledgement that the general relation between the electric displacement $\mathbf{D}$ and the electric field $\mathbf{E}$, given by the dielectric response tensor of the medium, $\epsilon(\mathbf{r}, \mathbf{r}', t - t')$, involves the response of the system not only at time t but also the delayed response to the field at previous times $t' < t$,

$$\mathbf{D}(\mathbf{r}, t) = \int \mathrm{d}\mathbf{r}' \int_{-\infty}^{t} \mathrm{d}t' \epsilon(\mathbf{r}, \mathbf{r}', t - t') \cdot \mathbf{E}(\mathbf{r}', t'). \tag{5.4.22}$$

The time integration can be rewritten as a temporal Fourier transform, and the response function replaced by the more familiar frequency-dependent electric permittivity, so that

$$\mathbf{D}(\mathbf{r}, t) = \int \mathrm{d}\mathbf{r}' \epsilon(\mathbf{r}, \mathbf{r}', \omega) \cdot \mathbf{E}(\mathbf{r}', \omega). \tag{5.4.23}$$

However, (5.4.22) also acknowledges that the response at a position $\mathbf{r}$ depends on positions within the locality of $\mathbf{r}$, as well as the point of measurement itself. Strictly speaking, this *non-locality* holds for all materials at the microscopic level, as they are made of atoms, and the phenomenological approximation of a continuous medium is no longer applicable on this length scale. As the wavelength of light is typically much larger than the interatomic distance, it is generally reasonable to assume that $\mathbf{E}(\mathbf{r}') \approx \mathbf{E}(\mathbf{r})$, yielding a local response

$$\mathbf{D}(\mathbf{r}, \omega) = \epsilon(\mathbf{r}, \omega) \cdot \mathbf{E}(\mathbf{r}, \omega). \tag{5.4.24}$$

Nevertheless, it has been shown that non-local effects must be considered in order to model the behaviour of the Casimir force at finite temperature [19], and it has also been noted that this approximation may fail close to the surface of a material [20, 21]. For a system that is translationally invariant, with a response depending on the separation $\mathbf{r} - \mathbf{r}'$, we may write a new permittivity function by taking a spatial Fourier transform with the wave vector $\mathbf{k}$, as well as a temporal Fourier transform with respect to time:

$$\epsilon(\mathbf{k}, \omega) = \int \mathrm{d}\mathbf{r}' \int_{-\infty}^{t} \mathrm{d}t' \epsilon(\mathbf{r} - \mathbf{r}', t - t') \cdot \mathbf{E}(\mathbf{r}', t'). \tag{5.4.25}$$

This non-local dependence is known as spatial dispersion, being formally similar to temporal dispersion. Properly, a complete model of dispersion requires the dielectric response of the medium to fall off to its free space (bare vacuum) magnitudes, for high values of frequency and wave number:

$$\lim_{k \to \infty} \epsilon(\mathbf{k}, \omega) = 1 \quad \text{and} \quad \lim_{\omega \to \infty} \epsilon(\mathbf{k}, \omega) = 1. \tag{5.4.26}$$

Importantly, if the response of the material falls off fast enough with high wave numbers, the stress tensor (5.2.1) may turn out to be finite after all. To examine this question, however, requires detailed empirical information about the material sample, or a sufficiently well-motivated theoretical model of dielectric, from which its high-wavenumber response can be modelled. Such probing questions into the detailed structure of macroscopic media are beyond the scope of this present study and seem unlikely to yield a fundamental solution: the Casimir energy of a system without spatial or temporal dispersion can be stated exactly, as we witnessed in the previous chapter, and the divergence of the stress does not arise from its temporally dispersive properties.

5.5 Summary Remarks

In this chapter we have examined the local behaviour of the regularised stress tensor commonly used in calculations of the Casimir force for a dielectric medium inhomogeneous in one direction. We have seen that the usual expression for the stress tensor is not finite anywhere within the medium, whatever the temporal dispersion or index profile, and that this divergence is unlikely to be removed by simply modifying the regularisation procedure. These findings hold for all magnetodielectric media.

From our investigation, it is clear that a calculation of (5.2.1) for a piecewise definition of an inhomogeneous medium does not represent an approximation to the continuous case. Our result is consistent with earlier findings,[16] and illustrates the generality of the problem of specifying the local value of the electromagnetic stress tensor at $T = 0\,\mathrm{K}$ when the material parameters vary continuously over space. Moreover, we identify a divergence of the local value of the stress tensor that cannot be removed by the procedure of regularisation usually advocated; it arises specifically due to the unphysical contribution of high wave numbers in the continuum limit. This problem does not seem to be widely appreciated in the literature. In [13] and in [22] reflection coefficients were similarly employed to determine the Casimir force in systems with increasingly refined inhomogeneous features, but the limits of the applicability of this technique were not commented on.

A continuously varying medium introduces arbitrarily small inhomogeneities into a system. A possible explanation for the divergence we have identified is that the Casmir force does not depend on such small-scale inhomogeneities, and a generally finite and physically meaningful result must be obtained by finding some simple modification to the existing regularisation procedure.

[16] In [9] the stress inside an inhomogeneous medium with a similar profile to (5.4.20) was determined using the exact Green function. However, it was infinite everywhere. An alternative regularisation was proposed, but this proved unsuccessful [4].

References

1. I.E. Dzyaloshinskii, E.M. Lifshitz, L.P. Pitaevskii, Adv. Phys. **10**, 165 (1961)
2. J.N. Munday, F. Capasso, V.A. Parsegian, Nature **457**, 170 (2009)
3. A.W. Rodriguez, F. Capasso, S.G. Johnson, Nat. Photonics **5**, 211 (2011)
4. W.M.R. Simpson, S.A.R. Horsley, U. Leonhardt, Phys. Rev. A **87**, 043806 (2013)
5. T.G. Philbin, New J. Phys. **12**, 123008 (2010)
6. T.G. Philbin, New J. Phys. **13**, 063026 (2011)
7. L.D. Landau, E.M. Lifshitz, *Quantum Mechanics* (Butterworth-Heinemann, Oxford, 2005)
8. E. M. Lifshitz and L. P. Pitaevskii, *Statistical Physics* (Butterworth-Heinemann, Oxford, 2003)
9. T.G. Philbin, C. Xiong, U. Leonhardt, Ann. Phys. **325**, 579 (2009)
10. U. Leonhardt, *Essential Quantum Optics* (Cambridge University Press, Cambridge, 2010)
11. L. P. Pitaevskii, *Electrodynamics of Energy Loss Spectroscopy in the Electron Microscope* (Springer, New York, 2011)
12. E.M. Lifshitz, Zh. Eksp. Teor. Fiz. **29**, 94 (1955)
13. C. Genet, A. Lambrecht, S. Reynaud, Phys. Rev. A **67**, 043811 (2003)
14. M. Born, E. Wolf, *Principles of Optics* (Cambridge University Press, Cambridge, 1999)
15. I.A. Shelykh, V.K. Ivanov, Int. J. Theor. Phys. **43**, 477 (2004)
16. M. Artoni, G.C. La Rocca, F. Bassani, Phys. Rev. E **72**, 046604 (2005)
17. S.M. Barnett, B. Huttner, R. Loudon, R. Matloob, J. Phys. B: At. Mol. Opt. Phys. **29**, 3763 (1996)
18. S. Scheel, L. Knöll, D.-G. Welsch, Phys. Rev. A **60**, 4094 (1999)
19. B.E. Sernelius, Phys. Rev. B **71**, 235114 (2005)
20. R. Esquivel-Sirvent et al., J. Phys. A: Math. Gen. **39**, (6323) (2006)
21. V.B. Svetovoy, R. Esquivel, Rev. E, **72**, 036113 (2005)
22. S. Ellingsen, J. Phys. A: Math. Theor. **40**, 1951 (2007)